

ANALYSIS OF ELECTROMAGNETIC FIELDS IN INHOMOGENEOUS MEDIA BY FOURIER SERIES EXPANSION METHODS – THE CASE OF A DIELECTRIC CONSTANT MIXED A POSITIVE AND NEGATIVE REGIONS

Tsuneki Yamasaki¹

¹ Department of Electrical Engineering, College of Science and Technology, Nihon University
yamasaki@ele.cst.nihon-u.ac.jp

Keywords: Inhomogeneous and negative medium, Improved Fourier series expansion, Electromagnetic wave.

Abstract: In this paper, we propose a new method for the electromagnetic fields with inhomogeneous media mixed the positive and negative regions which is the combination of improved Fourier series expansion method using the extrapolation method. Numerical results are given for the power reflection and transmission coefficient, the energy absorption, the electromagnetic fields, and the power flow in the inhomogeneous medium mixed the positive and negative regions including the case when the permittivity profiles touches zero for the TM wave. The results of our method are in good agreement with exact solution which is obtained by MMA.

1 INTRODUCTION

Recently, the scattering and guiding problems of the inhomogeneous media have been of considerable interest, such as optical fiber gratings, photonic bandgap crystals, frequency selective devices, and a negative medium (Caloz et al., 2004). In the negative medium, such as a plasma (Freidberg et al., 1972) or a metallic grating (Yasuura et al., 1986), the permittivity has both positive and negative regions.

One of the methods that are commonly employed in solving the problems in an inhomogeneous medium is the homogeneous multilayer approximation method (HMA). Although the method is widely known and is proved to solve the electromagnetic fields in inhomogeneous media, it cannot be applied to the positive and negative regions with oblique angle of incidences in TM wave.

Yamaguchi and Hosono (Yamaguchi et al., 1982) pointed out this difficulty and applied the modified multilayer approximation method (MMA) to this problem. However MMA cannot be applied to the case when the permittivity profiles touches zero. In

this case, HMA cannot also obtain the electromagnetic fields even if the loss term of the permittivity tends to zero.

In this paper, we propose a new method for the electromagnetic fields with inhomogeneous media mixed the positive and negative regions which is the combination of improved Fourier series expansion method (Yamasaki et al., 1984) using the extrapolation method.

K.F. Casey (Casey, 1972) has presented a Fourier series expansion method to get the rigorous solution in inhomogeneous media. However, they did not present any numerical results for the sinusoidally stratified plasma media whose permittivity had the only positive region (Casey et al., 1969).

Numerical results are given for the power reflection and transmission coefficient, the energy absorption, the electromagnetic fields, and the power flow in the inhomogeneous medium mixed the positive and negative regions including the case when the permittivity profiles touches zero for the TM wave. The results of our method are in good agreement with exact solution which is obtained by MMA.

2 METHOD OF ANALYSIS

We consider an inhomogeneous medium mixed the positive and negative regions as shown in Fig.1. The structure is uniform in the y -direction and the permittivity $\varepsilon_2(z)$ has zero at $z = z_1$ and $z = z_2$ (see Fig.1(b)). The permeability is assumed to be μ_0 . The time dependence is $\exp(-i\omega t)$ and suppressed throughout.

In the formulation, the TM wave (the magnetic field has only the y -component) is discussed. When the TM wave is assumed to be incident from $z < 0$ at the angle θ_0 , the magnetic fields in the regions $S_1 (z \leq 0)$ and $S_3 (z \geq d)$ are expressed (Yamasaki et al., 1984) as

$S_1 (z \leq 0)$:

$$H_y^{(1)} = e^{ik_1(x \sin \theta_0 + z \cos \theta_0)} + R e^{ik_1(x \sin \theta_0 - z \cos \theta_0)}, \quad (1)$$

$$k_1 \triangleq \omega \sqrt{\varepsilon_1 \mu_0} = k_0 \sqrt{\varepsilon_1 / \varepsilon_0}, \quad k_0 \triangleq 2\pi / \lambda,$$

$S_3 (z \geq d)$:

$$H_y^{(3)} = T e^{i\{k_1 x \sin \theta_0 + k_{3z}(z-d)\}}, \quad (2)$$

$$k_{3x} \triangleq \sqrt{k_3^2 - (k_1 \sin \theta_0)^2}, \quad j = 1, 3$$

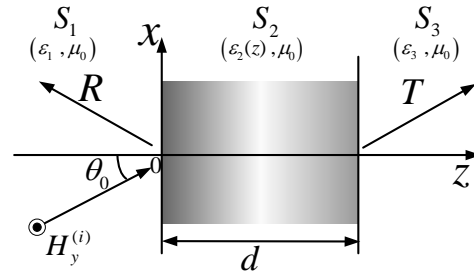
where λ is the wavelength in free space, R , and T are the reflection and transmission coefficient to be determined by boundary conditions.

The inhomogeneous layer ($0 < z < d$) consists of periodically stratified layers which is the iteration of the permittivity $\varepsilon_d(z) [= \varepsilon_2(z)]$ in the original region ($0 < z < d$; see Fig.2) (Yamasaki et al., 1984). The modal component of magnetic field can be written as $H_y^{(2)} = H(z) e^{ik_1 x \sin \theta_0}$, and $H(z)$ must satisfy the following wave equation (Yamasaki et al., 1984)

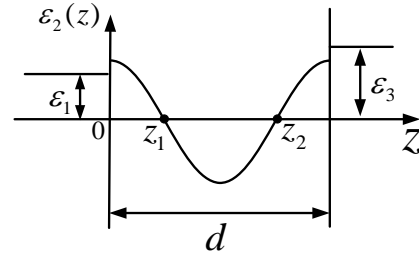
$$\frac{d^2 H(z)}{dz^2} - \frac{1}{\varepsilon_d(z)} \frac{d\varepsilon_d(z)}{dz} \frac{dH(z)}{dz} + [k_0^2 \varepsilon_d(z) / \varepsilon_0 - (k_1 \sin \theta_0)^2] H(z) = 0. \quad (3)$$

In the lossless case in $\varepsilon_d(z)$, the singularity appears in the second term in Eq.(3).

Taking into account the Floquet's theorem, $H(z)$ can be approximated by the finite Fourier series as



(a) Coordinate system



(b) Distribution of dielectric constant

Fig.1 Structure of the inhomogeneous medium mixed the positive and negative region.

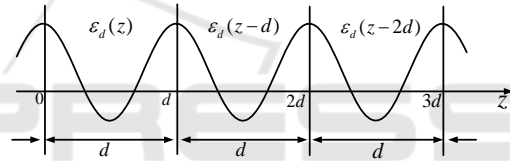


Fig 2. Periodically inhomogeneous layers

$$H(z) = e^{ihz} \sum_{n=-N}^N u_n e^{i2\pi n z / d} \quad (4)$$

To obtain the correct solution in the analysis of lossless case, $\varepsilon_d(z)$ is including the loss term σ (Yamasaki et al., 2004, 2005(a), (b))

$$\tilde{\varepsilon}_d(z) / \varepsilon_0 \triangleq \varepsilon_d(z) / \varepsilon_0 + i\sigma \quad (\sigma \geq 0). \quad (5)$$

Substituting Eqs.(5) and (4) into Eq.(3), and multiplying both side by $\tilde{\varepsilon}_d(z) e^{-i2\pi n z / d}$, and rearranging after integrating with respect to z in the interval $0 < z < d$. We get the following equation in regard to h (Yamasaki et al., 1984)

$$h^2 \mathbf{M} \mathbf{U} + h \mathbf{C} \mathbf{U} + \mathbf{K} \mathbf{U} = 0, \quad (6)$$

where

$$\mathbf{U}^{(t)} \triangleq [u_{-N}, \dots, u_0, \dots, u_N]^T, \quad T: \text{transpose}$$

$$\mathbf{M} \triangleq [\eta_{m,n}], \quad \mathbf{C} \triangleq [\zeta_{m,n}], \quad \mathbf{K} \triangleq [\gamma_{m,n}],$$

$$\zeta_{n,m} \triangleq \frac{2\pi}{d} \{2n + (n - m)\} \eta_{n,m},$$

$$\gamma_{n,m} \triangleq \left[\left(\frac{2\pi}{d} \right)^2 (n^2 + n(n-m)) + (k_0 \sin \theta_0)^2 \right] \eta_{n,m} - \xi_{n,m},$$

$$m, n = (-N, \dots, 0, \dots, N), \quad (7)$$

$$\eta_{n,m} \triangleq \frac{1}{d} \int_0^d \left\{ \tilde{\varepsilon}_d(z) / \varepsilon_0 \right\} e^{i2\pi(n-m)z/p} dz,$$

$$\xi_{n,m} \triangleq \frac{k_0^2}{d} \int_0^d \left\{ \tilde{\varepsilon}_d(z) / \varepsilon_0 \right\}^2 e^{i2\pi(n-m)z/p} dz.$$

Letting $\mathbf{V} \triangleq \mathbf{h}\mathbf{U}$ and modifying Eq.(6), it is reduced to the following conventional eigenvalue equation

$$\mathbf{A}\mathbf{W} = \mathbf{h}\mathbf{W}, \quad (8)$$

$$\mathbf{A} \triangleq \begin{bmatrix} \mathbf{0} & \mathbf{1} \\ -\mathbf{M}^{-1}\mathbf{K} & -\mathbf{M}^{-1}\mathbf{C} \end{bmatrix},$$

$$\mathbf{W} \triangleq \begin{bmatrix} \mathbf{U} \\ \mathbf{V} \end{bmatrix},$$

where $\mathbf{1}$ is unit vector and \mathbf{M}^{-1} is inverse matrix of \mathbf{M} .

When it gets an eigenvalue $h_0 (= \beta + i\alpha; \alpha \geq 0)$ obtained Eq.(8) for $N \rightarrow \infty$, $-h_0 (= -\beta - i\alpha)$ is the solution, and $(\pm h_0 \pm 2\pi n/d)$ are also solutions (Yamasaki et al., 1984). Therefore we selected h_0 by convergence characteristics of $(\pm h_0 \pm 2\pi n/d)$ in section of numerical analysis.

In the lossless case for $\sigma \rightarrow 0$, we can get the eigenvalue h_{EV} according to the following extrapolation equation ($a_0 \triangleq h_{EV}$) in regard to the loss parameters $\sigma_j (j=1 \sim 3)$ (Yamasaki et al., 2004, 2005(a), (b))

$$h_0(\sigma_j) = a_0 + a_1 \cdot \sigma_j + a_3 \cdot (\sigma_j)^2; j = 1 \sim 3. \quad (9)$$

In the same manner, the eigenvectors $u_n^{(EV)}$ are also obtained by the following extrapolation equation ($b_0 \triangleq u_n^{(EV)}$) in regard to the loss parameters $\sigma_j (j=1 \sim 3)$ (Yamasaki et al., 2004, 2005(a), (b))

$$u_n^{(EV)}(\sigma_j) = b_0 + b_1 \cdot \sigma_j + b_3 \cdot (\sigma_j)^2; j = 1 \sim 3 \quad (10)$$

$S_2(0 < z < d)$:

Using h_{EV} and $-h_{EV}$, and the corresponding eigenvectors $u_n^{(EV)}$ and $u_n^{(-EV)}$, the electromagnetic fields in the inhomogeneous layer ($0 < z < d$) are expanded by a finite Fourier series (Yamasaki et al.,

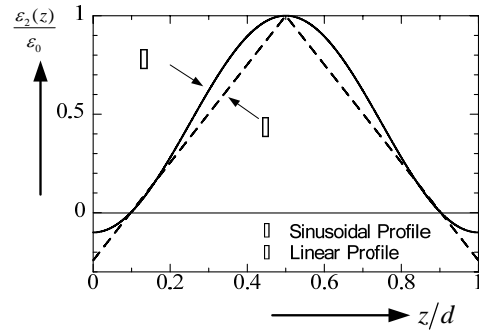
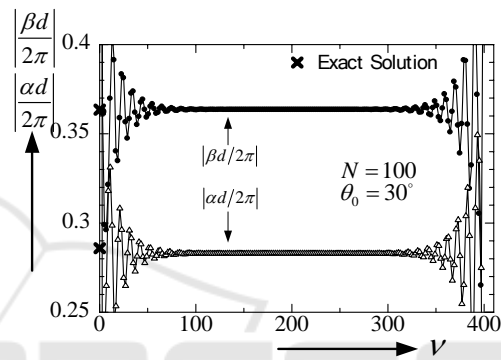
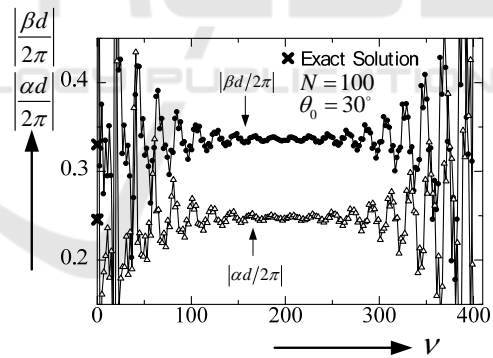


Fig.3 A profile of ① Eq.(15) and ② Eq.(16)



(a) Sinusoidal Profile case



(b) Linear Profile case

Fig.4 $|\beta d/2\pi|$ and $|\alpha d/2\pi|$ vs. ν

2004, 2005(a), (b))

$$H_y^{(2)} = e^{ik_1 \sin \theta_0 x} [t_v^{(2)} e^{ih_{EV}z} f_{EV}(z) + r_v^{(2)} e^{-ih_{(-EV)}z} f_{(-EV)}(z)], \quad (11)$$

$$f_{EV}(z) \triangleq \sum_{n=-N}^N u_n^{(EV)} e^{i\frac{2\pi n}{d}z},$$

$$f_{(-EV)}(z) \triangleq \sum_{n=-N}^N u_n^{(-EV)} e^{i\frac{2\pi n}{d}z},$$

$$E_x^{(2)} = \{-i\omega \varepsilon(z)\}^{-1} \partial H_y^{(2)} / \partial z, \quad (12)$$

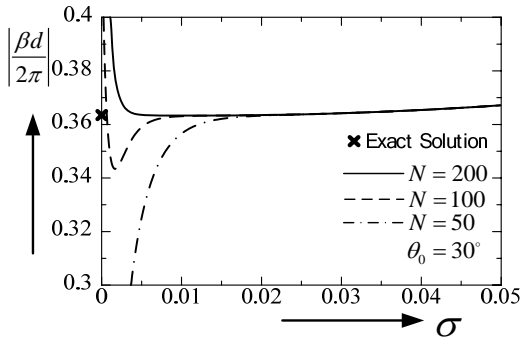
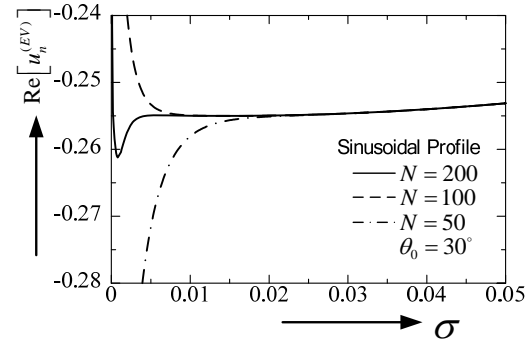
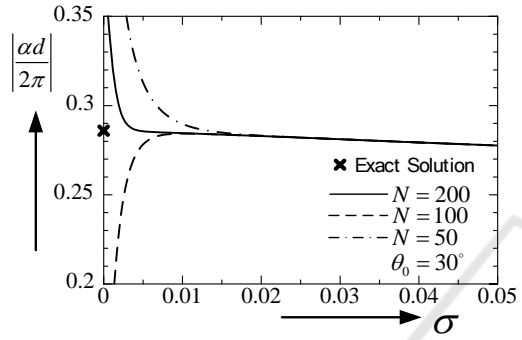

 (a) $|\beta d/2\pi|$

 (a) $\text{Re}[u_n^{(EV)}]$

 (b) $|\alpha d/2\pi|$

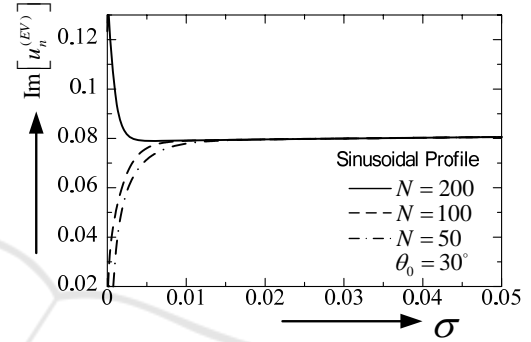
 Fig.5 $|\beta d/2\pi|$ and $|\alpha d/2\pi|$ vs. σ

 (b) $\text{Im}[u_n^{(EV)}]$

 Fig.6 $\text{Re}[u_n^{(EV)}]$ and $\text{Im}[u_n^{(EV)}]$ vs. σ

where, $t_v^{(2)}$ and $r_v^{(2)}$ are unknown coefficients which satisfy the boundary conditions.

Using the boundary conditions and $T(=T_{EV})$ can be obtained by (the following equation):

$$R_{EV}(N) = T_{EV}(N) - 1,$$

$$T_{EV}(N) = 2[f_{EV}(d)D - f_{(-EV)}(d)C] / (AD - CD), \quad (13)$$

where,

$$\begin{aligned} A &\triangleq f_{EV}(0) + \frac{\varepsilon_1 F_1}{\varepsilon_d(0)k_1 \cos \theta_0}, \\ B &\triangleq f_{(-EV)}(0) + \frac{\varepsilon_1 F_2}{\varepsilon_d(0)k_1 \cos \theta_0}, \\ C &\triangleq f_{EV}(d) - \frac{\varepsilon_3 F_1}{\varepsilon_d(d)k_{3x}} e^{ih_{EV}d}, \\ D &\triangleq f_{(-EV)}(d) - \frac{\varepsilon_3 F_2}{\varepsilon_d(d)k_{3x}} e^{-ih_{EV}d} \end{aligned} \quad (14)$$

$$F_1 \triangleq \sum_{n=-N}^N \left(\frac{2\pi n}{d} + h_{EV} \right) u_n^{(EV)},$$

$$F_2 \triangleq \sum_{n=-N}^N \left(\frac{2\pi n}{d} - h_{EV} \right) u_n^{(-EV)}.$$

3 NUMERICAL ANALYSIS

We consider the following two profiles (see Fig.3):

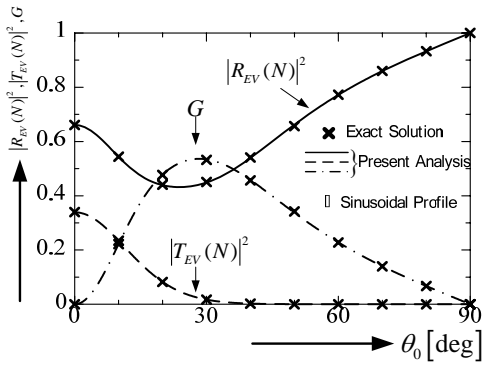
(1) Sinusoidal profile:

$$\varepsilon_2(z) / \varepsilon_0 = \varepsilon_A \{1 - \delta \cos(2\pi z / d)\} \quad (15)$$

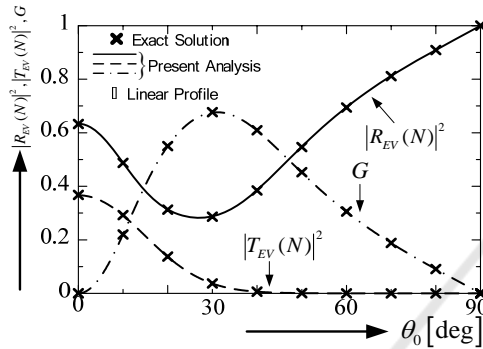
(2) Linear profile:

$$\frac{\varepsilon_2(z)}{\varepsilon_0} = \begin{cases} \varepsilon_2(\min) + [\varepsilon_2(\max) - \varepsilon_2(\min)] \frac{2}{d} z : 0 < z \leq \frac{d}{2} \\ \varepsilon_2(\min) + [\varepsilon_2(\max) - \varepsilon_2(\min)] \frac{2}{d} (z - d) : \frac{d}{2} \leq z < d \end{cases} \quad (16)$$

where,



(a) Sinusoidal Profile case



(b) Linear Profile case

 Fig.7 $|R_{EV}(N)|^2$ and $|T_{EV}(N)|^2$ and G^2 vs. θ_0

$$\varepsilon_A \triangleq \frac{[\varepsilon_2(\max) + \varepsilon_2(\min)]}{2},$$

$$\delta \triangleq \frac{[\varepsilon_2(\max) - \varepsilon_2(\min)]}{[\varepsilon_2(\max) + \varepsilon_2(\min)]},$$

It has two zero points at $z_1/d \cong 0.0975$ and $z_2/d \cong 0.9025$ for both profiles. The values of parameters chosen are $\varepsilon_1 = \varepsilon_3 = \varepsilon_0$, $\varepsilon_2(\max) = 1$ and $\sqrt{A}\lambda/d = 0.8$. $\varepsilon_2(\min) = -0.1$ is the sinusoidal case and $\varepsilon_2(\min) \cong -0.242236$ is the linear case.

Figures 4(a) and 4(b) show the convergence of complex propagation constants $|\beta d/(2\pi)|$ and $|\alpha d/(2\pi)|$ to normalize $h_{EV} (= \beta + i\alpha)$ with $N = 100$, $\sigma = 0.01$, and $\theta_0 = 30^\circ$ for the mode number $\nu = 1 \sim 2(2N + 1)$. In these Figures, cross points (x) are the exact solution which is obtained by the following characteristic equation in regard to h (Hosono, 1973)

$$\cos(hd) = (A_S + D_S)/2, \quad (17)$$

where, A_S and D_S are the following Matrix

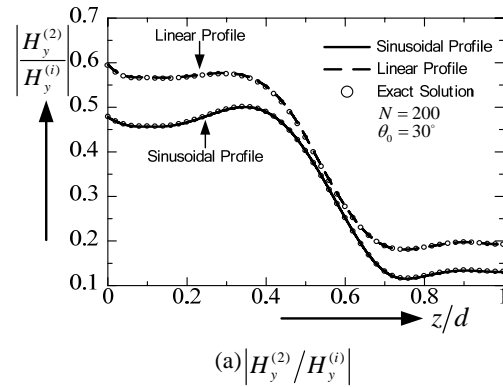
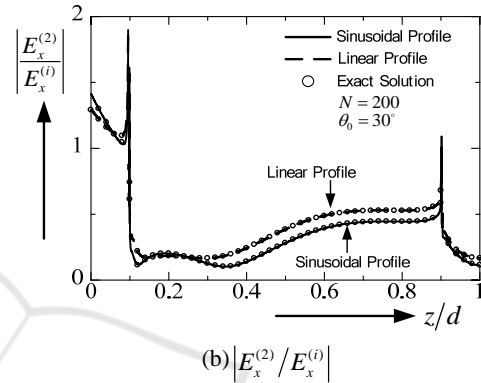

 (a) $|H_y^{(2)}/H_y^{(i)}|$

 (b) $|E_x^{(2)}/E_x^{(i)}|$

 Fig.8 $|H_y^{(2)}/H_y^{(i)}|$ and $|E_x^{(2)}/E_x^{(i)}|$ vs. z/d

elements can be written using the Floquet's theorem

$$\begin{bmatrix} H_y^{(2)} \\ E_x^{(2)} \end{bmatrix}_{z=0} = \begin{bmatrix} A_S & B_S \\ C_S & D_S \end{bmatrix} \begin{bmatrix} H_y^{(2)} \\ E_x^{(2)} \end{bmatrix}_{z=d} \quad (18)$$

$$= e^{\mp jhd} \begin{bmatrix} H_y^{(2)} \\ E_x^{(2)} \end{bmatrix}_{z=d}$$

In Eq.(18), the magnetic fields $H_y^{(2)}$ are expanded by a finite power series (Budden, 1961) which are approximated by the linear profile including $\varepsilon_2(z) = 0$ as follows (Yamaguchi et al., 1982, Budden, 1961):

$$H_y^{(2)} \triangleq e^{ik_1 \sin \theta_0 x} [t_v^{(2)} w_1(Z) + r_v^{(2)} w_2(Z)], \quad (19)$$

where

$$Z \triangleq \left(\frac{k_0^2}{\varepsilon_0 d \varepsilon_2(z) / dz} \right)^{2/3} \cdot \varepsilon_2(z),$$

$$w_1(Z) = \sum_{n=0}^M a_n Z^n; \quad a_0 = 1, a_1 = 0, a_n = \frac{cb_{n-2} - b_{n-3}}{n(n+2)};$$

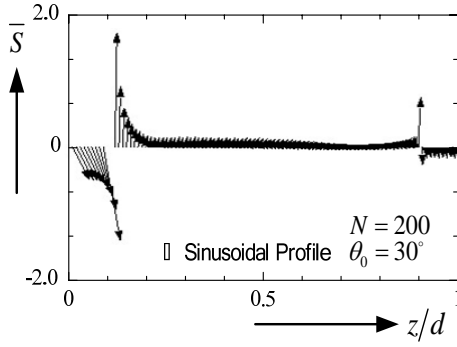
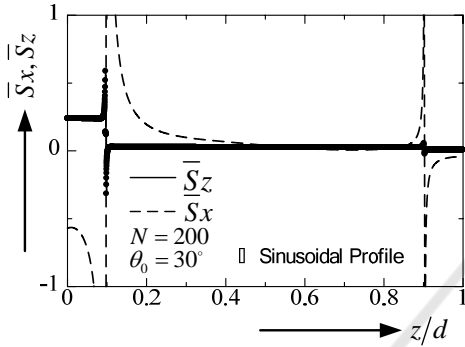

 (a) Poynting Vector \bar{S}

 (b) Poynting Vector \bar{S}_x, \bar{S}_z

Fig.9 Poynting Vector of Sinusoidal Profile

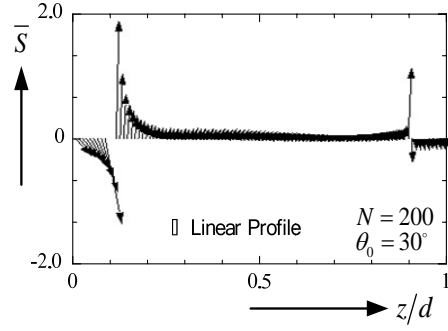
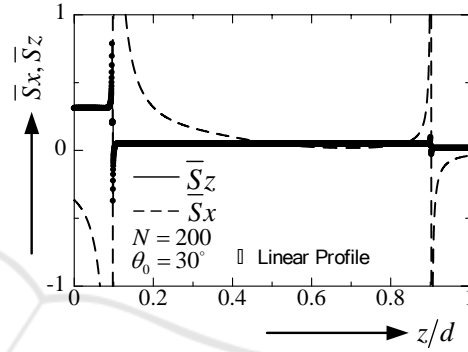

 (a) Poynting Vector \bar{S}

 (b) Poynting Vector \bar{S}_x, \bar{S}_z

Fig.10 Poynting Vector of Linear Profile

$$w_2(Z) = \left(\frac{c}{2} \log Z\right) w_1(Z) + \sum_{n=0}^M b_n Z^n; \quad b_0 = 1, b_1 = 0, b_2 = 0,$$

$$b_n = \frac{cb_{n-2} - b_{n-3} - c(n-1)}{n(n-2)}; \quad c = k_0^2 \sin^2 \theta_0 / (k_0^2 d \varepsilon_2(z) / dz)^{2/3}.$$

From Figure 4, the modal number chosen is $\nu = 2N + 1$ ($=201$) gives good convergence in comparison with the exact solution which is obtained for $M = 1000$ in Eq.21. The values of exact solution are $|\beta d / (2\pi)| \cong 0.3635$ and $|\alpha d / (2\pi)| \cong 0.2859$ for the sinusoidal profile, and $|\beta d / (2\pi)| \cong 0.3303$ and $|\alpha d / (2\pi)| \cong 0.2454$ for the linear profile. The convergence tendency of the sinusoidal profile is faster than that of the linear profile. Figures 5(a) and 5(b) show the $|\beta d / (2\pi)|$ and $|\alpha d / (2\pi)|$ for various values of loss term σ at the modal number $\nu (= 2N + 1)$ in the sinusoidal profile. The results of the present method seem to be difficult when σ tends to zero for increasing modal truncation number N , but the true value can be obtained by extrapolation method.

Figures 6(a) and 6(b) show the eigenvectors $u_n^{(EV)}$ ($\text{Re}[u_n^{(EV)}]$ and $\text{Im}[u_n^{(EV)}]$) for various values of loss term σ at the same conditions as in Fig.5 for the sinusoidal profile. From Figure 6, the true value of the eigenvectors $u_n^{(EV)}$ can be obtained by the extrapolation method for $N \geq 200$. On the other hand, the case of linear profile, the convergence tendency is slower than that of sinusoidal profile. But the extrapolation method is also effective for $N \geq 200$.

Figures 7(a) and 7(b) show the power reflection coefficient $|R_{EV}(N)|^2$, the power transmission coefficient $|T_{EV}(N)|^2$, and the power loss of energy difference $G[\triangleq 1 - |R_{EV}(N)|^2 - |T_{EV}(N)|^2]$ for various values of incident angle θ_0 using the extrapolation method to select the loss term at $\sigma_1 = 0.01$, $\sigma_2 = 0.02$, and $\sigma_3 = 0.03$. The results of the present method are in good agreement with those of exact solutions. The relative error to the exact

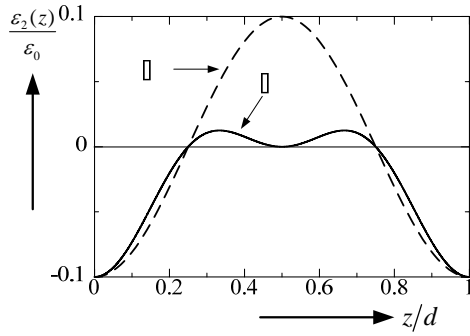
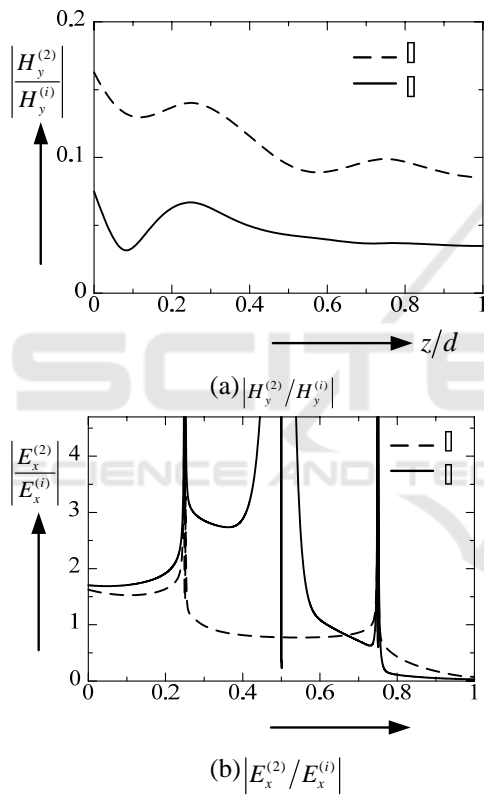


Fig.11 A profile of ① Eq.(16) and ②Eq.(22)


 Fig.12 $|H_y^{(2)}/H_y^{(i)}|$ and $|E_x^{(2)}/E_x^{(i)}|$ vs. z/d

solutions is about 0.02% for the sinusoidal profile and 0.2% for the linear profile when the modal truncation number chosen is $N = 200$. From Figure 7, the energy absorption G is nonzero even if the medium is lossless case.

Figures 8(a) and 8(b) show the normalized magnetic fields $|H_y^{(2)}/H_y^{(i)}|$ and the normalized electric fields

$|E_x^{(2)}/E_x^{(i)}|$ for various values of z/d at $\theta_0 = 30^\circ$ for $N = 200$ using the extrapolation method in Fig.5 and Fig.6. From Fig.8, the results of the present method are in good agreement with those of exact solutions. In the sinusoidal case, $|H_y^{(2)}/H_y^{(i)}|$ is about constant rather than that of the linear case in $0 \leq z/d < 0.4$. This is attributed to the effect of the profile and the angle of incidence θ_0 .

On the other hand, the characteristic tendency of $|E_x^{(2)}/E_x^{(i)}|$ is about same in both profiles, and the effects of singularities are clearly seen at $z_1/d \cong 0.0975$ and 0.9025 , but it has the limited value at this point because of $\partial H_y^{(2)}(z_1 \text{ or } z_2)/\partial z = 0$,

$$f_E(z) \triangleq |E_x^{(2)}/E_x^{(i)}| \\ = \lim_{z \rightarrow z_1, z_2} \left| \frac{\partial H_y^{(2)}(z)/\partial z}{d\varepsilon_2(z)/dz} \right|. \quad (20)$$

In the Fig.8(b), the limiting values are $f_E(z_1) \cong 0.6096$ and $f_E(z_2) \cong 0.4152$.

Figures 9 and 10 show the Poynting vectors of \bar{S} , \bar{S}_x , and \bar{S}_z for various values of z/d in the inhomogeneous region with the same parameters as in Fig.8 for both profiles. The definition of Poynting vector is as follows:

$$\bar{S} = \bar{S}_x \mathbf{i} + \bar{S}_z \mathbf{j}, \\ \bar{S}_x \triangleq -\text{Re}[E_z \times H_y^*]/2, \\ \bar{S}_z \triangleq \text{Re}[E_x \times H_y^*]/2. \quad (21)$$

where, \mathbf{i} and \mathbf{j} are unit vectors in the direction of x axis and z axis, respectively.

From Figs.9 and 10, we see the following features:

(1) The effect of a positive and negative medium are more significant at $z_1/d \cong 0.0975$ and $z_2/d \cong 0.9025$, so that the direction reverses to the power flow \bar{S} at that points.

(2) In the sinusoidal case, \bar{S}_z has the limited values at points of zeros $z_1/d \cong 0.0975$ and $z_2/d \cong 0.9025$, so that $\bar{S}_z(z_1) \cong 0.1300$ and $\bar{S}_z(z_2) \cong 0.0166$, respectively.

On the other hand, $\bar{S}_z(z_1) \cong 0.21245$ and $\bar{S}_z(z_2) \cong 0.03396$ at those points for the linear case. The energy of these points are absorbed.

(3) \bar{S}_x becomes infinite and the sign is reversed at the singularities $z_1/d \cong 0.0975$ and $z_2/d \cong 0.9025$.

In the investigation of above results, our methods can be applied to the positive and negative medium and have good accuracy of the electromagnetic fields.

So, next we consider the distribution of permittivity $\varepsilon_2(z)$ touches $\varepsilon_2(z)=0$. This problem is difficult to analyze by the MMA.

We consider the following sinusoidal profile② (see Fig.(11))

$$\varepsilon_2(z) / \varepsilon_0 = \varepsilon_A \{0.5 - \delta \cos(2\pi z / d) + 0.5 \cos(4\pi z / d)\}. \quad (22)$$

It has three zero points at $z_1/d = 0.25$, $z_2/d = 0.5$, and $z_3/d = 0.75$. The definition of ε_A and δ are the same in Eq.(16). The values of parameters chosen are $\varepsilon_1 = \varepsilon_3 = \varepsilon_0$, $\varepsilon_2(\max) = 0.1$ (profile ①), $\varepsilon_2(\max) = 0$ (profile ②), $\varepsilon_2(\min) = -0.1$ and $\sqrt{A}\lambda/d = 0.8$.

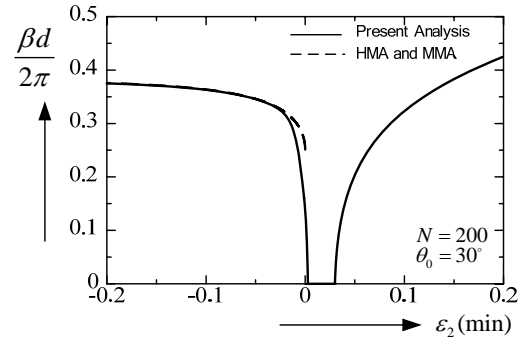
Figures 12(a) and 12(b) show the normalized magnetic fields $|H_y^{(2)}/H_y^{(i)}|$ and the normalized electric fields $|E_x^{(2)}/E_x^{(i)}|$ for various values of z/d at $\theta_0 = 30^\circ$ comparison with the profile ① in Eq.(16) for $N = 200$ using the extrapolation method.

From in Fig.(12), we see the following features:

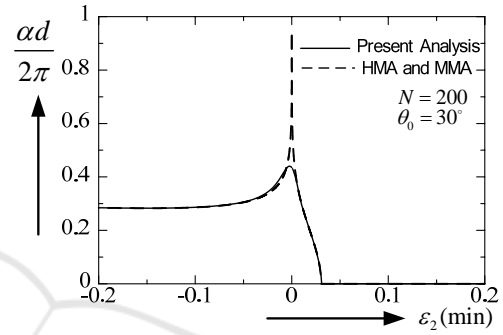
- (1) For the $|H_y^{(2)}/H_y^{(i)}|$, the influence of distribution of profiles ① and ② appears over $z/d = 0.5$,
- (2) The effect of the distribution of permittivity $\varepsilon_2(z)$ which touches $\varepsilon_2(z)=0$ is more significant of the electric fields $|E_x^{(2)}/E_x^{(i)}|$ at $z_2/d = 0.5$, and the limiting values are $f_E(z_1) \cong 3.2904$, $f_E(z_2) \cong 0.35798$ and $f_E(z_3) \cong 0.65633$ for the profile ②. In the case of ①, there are

$$f_E(z_1) \cong 1.1417 \text{ and } f_E(z_3) \cong 0.77027.$$

Finally, we investigate the complex propagation constants in the periodically inhomogeneous layers



(a) $\beta d/2\pi$



(b) $\alpha d/2\pi$

Fig.13 $\beta d/2\pi$ and $\alpha d/2\pi$ vs. $\varepsilon_2(\min)$

changing $\varepsilon_2(\min)/\varepsilon_0$ in the case of fixed $\varepsilon_2(\max)/\varepsilon_0 = 1.0$ in Eq.(16).

Figures 13(a) and 13(b) show the $\beta d/(2\pi)$ and $\alpha d/(2\pi)$ for various values of $\varepsilon_2(\min) = -0.1 \sim 0.1$ at $\theta_0 = 30^\circ$ for $N = 200$ using the extrapolation method.

In this figure, the dashed line (---) are the results of MMA ($\varepsilon_2(\min) < 0$) and HMA ($\varepsilon_2(\min) > 0$). Both methods cannot be applied to the $\varepsilon_2(\min) = 0$. From in Fig.13, the results of MMA and HMA are not accurate at $\varepsilon_2(\min) = 0$, because the normalized attenuation constant $\alpha d/(2\pi)$ in this case appears $\varepsilon_2(\min)/\varepsilon_0 \leq 0.0295$.

4 CONCLUSIONS

In this paper, The Fourier series expansion method is applied to the electromagnetic fields with inhomogeneous media mixed the positive and negative regions using the extrapolation method

which obtains the correct value of the eigenvalue and eigenvectors for the case of TM wave.

Numerical results are given for the power reflection and transmission coefficient, the energy absorption, the electromagnetic fields, and the power flow in the inhomogeneous medium mixed the positive and negative regions including the case of the permittivity profiles touches zero for the case of the TM wave. The results of our method are in good agreement with exact solution which is obtained by MMA.

Yasuura K., Murayama M., 1986, *Numerical Analysis of Diffraction from a Sinusoidal Metal Grating*, IEICE Trans., Vol.J69-B, no2, pp.198-205 (in Japanese).

REFERENCES

Budden K.C., 1961, *Radio Waves in the Ionosphere*, Cambridge Univ., Press, pp.343-347.

Caloz C. , Itoh T.,2004, *Microwave Application of Metamaterial Structures*, IEICE Technical Report. Vol.104, No202, pp135-138.

Casey K.F., Matthes J.R. and Yeh C. ,1969, *Wave Propagation in Sinusoidally Stratified Plasma Media*, J.Math.Phys., Vol.10, no5, pp.891-896.

Casey K.F.,1972, *Application of Hill's Function to problem of propagation in Stratified Media*, IEEE Tran.Antenas Propagt. ,vol.AP-20, 3, p.369-374.

Freidberg J.P., Mitchell R.W., Morse R.L. , *Rudinski L.I.*,1972,*Resonant Absorption of Laser Light by Plasma Targets*, Phys. Rev. Lett.,Vol.28,no13.,pp.795-799.

Hosono T.,1973, *Fundation of Electromagnetic Wave Engineering*, p.247, Shioko Publ. Co.(in Japanese) .

Yamaguchi S., Hosono T.,1982, *Some Difficulties in Homogeneous Multilayer Apporoximation Method and Their Remedy*, IEICE Trans.,Vol.J64-B, no10, pp.1115-1122 (in Japanese 1981) [translated Scripta Technica, INC., Vol.65-B, No.5 pp.75-83.

Yamasaki,T ,Hinata T.,Hosono H., 1984, *Analysis of Electrogagnetic Field in inhomogeneous Media by Foirier Series Expansion Methods*, IEICE Trans. Vol.J66-B, no10., pp.1239-1246(in Japanese 1983) [translated Scripta Technica, INC., Vol.67-B, No.6, pp.61-71.

Yamasaki t.,Isono K.,Hinata T., 2004, *Analaysis of Electromagnetic Field in Inhomogeneous media by Fourier Series Expansion Method -The case of a dielectric constant mixed in positive/negative medium* , Part I ,IEE Technical Reports Japan, EMT-04-121, pp.31-36(in Japanese) .

Yamasaki t.,Isono K.,Hinata T., 2005(a), *Analaysis of Electromagnetic Field in Inhomogeneous media by Fourier Series Expansion Method -The case of a dielectric constant mixed in positive/negative medium*, Part II, IEE Technical Reports Japan, EMT-05-7, pp.35-40 (in Japanese) .

Yamasaki T., Isono K., Hinata T., 2005(b), *Analaysis of Electromagnetic Fields in Inhomogeneous media by Fourier Series Expansion Method -The case of a dielectric constant mixed a positive and negative regions*, IEICE Trans. on Electronics, Vol.E88-C, No.12, pp.2216-2222.